

# Page-Based Weighted Bit-Flipping Decoding of Product LDPC Codes for Two-Dimensional Magnetic Recording

Sirawit Khittiwitayakul<sup>1</sup>, Watid Phakphisut<sup>2</sup> and Pornchai Supnithi<sup>3</sup>

<sup>1,2,3</sup> Faculty of Engineering, King Mongkut's Institute of Technology Ladkrabang, Bangkok 10520, Thailand

<sup>2</sup> Faculty of Science and Technology, Bangkok Suvarnabhumi University, Bangkok 10520, Thailand

E-mail: <sup>1</sup>57601155@kmitl.ac.th, <sup>2</sup>phwatid@gmail.com, <sup>3</sup>pornchai.su@kmitl.ac.th

**Abstract:** In this work, the performance of product LDPC codes with page-based weighted bit-flipping (P-WBF) decoding is evaluated on the two-dimensional magnetic recording (TDMR) channel of which areal density approaching 5.62 Tb/in<sup>2</sup>. Furthermore, we propose to use multiple bits flipping to improve the decoding speed of P-WBF algorithm. The number of bits flipped can be a constant or inconstant at each iteration decoding. The simulation results show that the performance of P-WBF with multiple bits flipping is better than those of the P-WBF algorithm at small iteration number. However, its performance will suffer at high iteration.

**Keywords**—Low density parity-check codes, Weighted bit-flipping, Two dimensional magnetic recording.

## 1. Introduction

Two-dimensional magnetic recording (TDMR) [1] is a promising technology to increase the areal density of hard-disk drive (HDD). TDMR differs from future novel storage such as heat-assisted magnetic recording (HAMR) [2] and bit-patterned media (BPM) [3] in that the media do not need to be redesigned. TDMR can use conventional head and media and relies on the powerful coding and signal processing. The readback signal of TDMR can be viewed as a two-dimensional (2-D) system. Therefore, the 2-D signal processing technique has recently received much attention [6-8].

A product low-density parity check (product LDPC) code [4] is two-dimensional (2-D) LDPC code whose performance is comparable to one-dimensional (1-D) LDPC code. It requires 2-D data bits for the encoding and decoding process. Therefore, the product LDPC code is suitable for 2-D signal processing of TDMR. In [5], the page-based weighted bit-flipping (P-WBF) decoding, which is the hard decision decoding algorithm for product LDPC codes, have been proposed. This algorithm flips the most unreliable bit based on the magnitudes of received signals. Although the P-WBF decoding gives worse performance than optimal soft-output belief-propagation (BP) decoding [10], it requires lower decoding complexity. The multiplication and division operations are not required for the P-WBF in contrast to the BP decoding.

In this work, we will increase the decoding speed of the P-WBF algorithm by flipping multiple bits at each iteration. We propose two methods to flip multiple bits. In the first method, the same number of bits is flipped at each iteration. We coined the term *page-fixed weighted bit-flipping (PF-WBF) algorithm*. In the second one, the number of flipped bits will be change following the threshold at each iteration. We coined the term *page-threshold weighted bit-flipping (PT-WBF) algorithm*. The performances of P-WBF, PF-

WBF and PT-WBF algorithms will be investigated in the additive write gaussian noise (AWGN) and TDMR channels. The rest of this paper is organized as follow. In Section 2 and 3, we explain the basics of TDMR channel and the P-WBF decoding algorithm, respectively. Then, we describe the proposed algorithms, i.e., PF-WBF and PT-WBF algorithm in Section 4. The simulation results and the conclusions are described in Section 5 and 6, respectively.

## 2. Two-dimensional magnetic recording

The TDMR modeling consist of 3 steps. In the first step, the recording media are generated similar to [6]. Then, in the second step, the data bits are recorded on the recording media. Finally, the readback signals are read from the media by using the parameters similar to [7-8]. The details of each step are explained as follow.

### 2.1. The four-grain media model

The recording media of TDMR is built from a granular material, which consists of a various grain sizes. In [6], the four-grain media model has been proposed to generate the granular material of TDMR. The discrete four-grain sizes have the dimensions of 1×1, 1×2, 2×1 and 2×2 with the corresponding probability of 33.33%, 25%, 25% and 16.67%, respectively. An example of the granular material built from the discrete four-grain as shown in Fig.1.

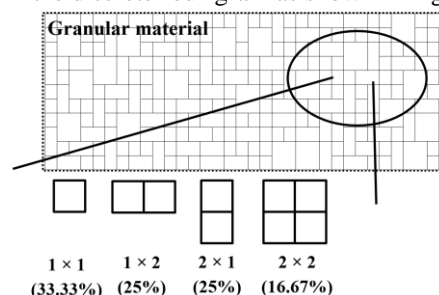


Fig. 1. An example of granular media with four-grain types.

### 2.2. Writing process

At the writing process, the data bits are modulated to the write current, then it is sent to the coil (at a gap between the write head and a recording media) to obtain the magnetic write field. The data bits are recorded on each grain of which the magnetization correspond to the recorded data. The grain size of 4×3 is used for one bit recording as shown in Fig. 2. We will use the parameters for one bit cell similar to [6], where the along-track ( $T_p$ ) and the cross-track length ( $L_b$ ) are set to 22 nm and 16.5 nm including the non-magnetic grains boundary, respectively. The areal density is equal 5.62 Tb/in<sup>2</sup>.

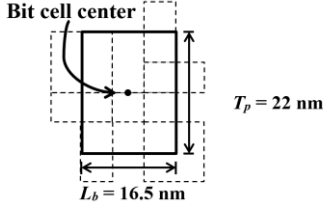


Fig. 2. the grain size of  $4 \times 3$  that are used for one bit recording.

### 2.3. Reading process

The reading process is the most important part since it is the recoverable process of the data bits. In [7], the geometry parameters  $H$ ,  $G$ ,  $T$ ,  $U$ ,  $h_m$ ,  $t_m$  and  $t_s$  denote the width between side shields, the shield gap, the width and thickness of magnetic recording (MR) element, the magnetic spacing, the thickness of recording layer and the thickness of intermediate layer, respectively. The closed-form representation of double-shielded reader sensitivity function is given by

$$\psi(x, y) = \alpha_0 \left\{ \tanh(\alpha_1 x + \alpha_2) - \tanh(\alpha_1 x - \alpha_2) \right\} \times \left\{ \tanh(\alpha_3 y + \alpha_4) - \tanh(\alpha_3 y - \alpha_4) \right\} \quad (1)$$

The  $x$  [nm] and  $y$  [nm] are the along-track and cross-track coordinates of one bit reading, respectively, where  $x = 0$  and  $y = 0$  represent the coordinates of bit cell center. The fitting parameters  $\alpha_k$  ( $k = 0, 1, \dots, 4$ ) represent the combination of the read head and recording media parameters i.e.,

$$\alpha_k = |w_{k0}H + w_{k1}G + w_{k2}T + w_{k3}U + w_{k4}h_m + w_{k5}t_m + w_{k6}t_s + w_{k7}| \quad (2)$$

The  $8 \times 5$  weight matrix  $\mathbf{w} = (\mathbf{w}_0^t, \mathbf{w}_1^t, \mathbf{w}_2^t, \mathbf{w}_3^t, \mathbf{w}_4^t)$  is investigated and optimized by real-coded genetic algorithm (RCGA) [8], where  $H$ ,  $G$ ,  $T$ ,  $U$ ,  $h_m$ ,  $t_m$  and  $t_s$  are set to 26, 15, 13, 2, 4, 10 and 1 nm, respectively. Figure 3 shows the pulse response for the reading process. The vertex of curve with the highest magnetization intensity represents the center of recorded bit. The magnetization intensity is decreased as the position is away from the bit cell center. Therefore, the inter-symbol interference (ISI) and inter-track interference (ITI) will occur because the pulse response influences more than 1 bit cell or  $4 \times 3$  grain size.

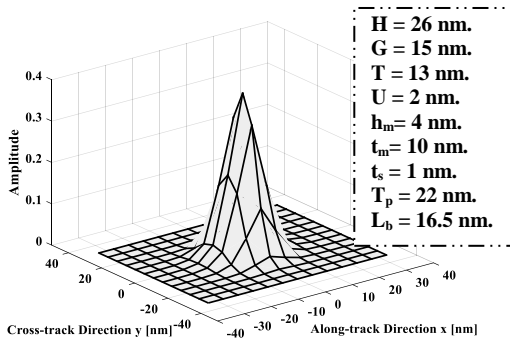


Fig. 3. the pulse response of reading process.

The read channel of TDMR is shown in Fig. 4. When the read back signals are read from the media, the amplitudes of the read back signals are disturbed by the thermal electronic noise. The high-frequency components of the read back signals are filtered by the low-pass filter

(LPF) and sampled to be the discrete sequence. The ISI and ITI components are handled by a partial response maximum likelihood (PRML) detector which consists of minimum mean-square error (MMSE) equalizer and soft-output Viterbi (SOVA) detector. Finally, the discrete sequence is decoded by LDPC decoder to recover the data bits.

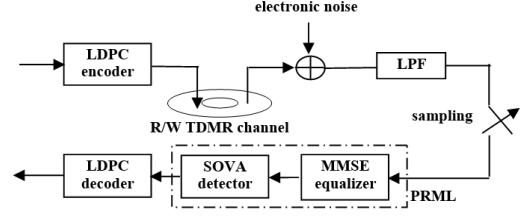


Fig. 4. the block diagram of PRML systems with TDMR channel.

### 3. Page-based weighted bit-flipping (P-WBF)

Recently, the P-WBF algorithm [5], a modification of the weighted bit-flipping algorithm [11], has been proposed for product LDPC codes or 2-D LDPC codes. Given that the 2-D information  $\mathbf{m}$  is encoded on row and column directions to obtain the 2-D codeword  $\mathbf{c}$ , where  $K^r \times K^c$  and  $N^r \times N^c$  are the sizes of 2-D information and 2-D codeword, respectively. The product LDPC codes have a parity-check matrix  $\mathbf{H}^{\text{row}}$  and  $\mathbf{H}^{\text{col}}$  that represent the relationship among the codeword bits on each row and column, respectively. Let  $N_{\text{row}}(m)$  and  $M_{\text{row}}(n)$  denote a set of non-zero positions in the  $m$ -th row and  $n$ -th column of  $\mathbf{H}^{\text{row}}$ , respectively. Similarly,  $N_{\text{col}}(m)$  and  $M_{\text{col}}(n)$  that represent a set of non-zero positions of  $\mathbf{H}^{\text{col}}$ . Let  $i$  and  $j$  be the row and column indices of each 2-D codeword, at the transmitter, the codeword bits  $c_{i,j}$  are modulated to the transmitted bits  $x_{i,j}$ , where  $x_{i,j} = 2c_{i,j} - 1$ . At the receiver, the received sequence  $\mathbf{y}$  is derived from  $\mathbf{y} = \mathbf{x} + \mathbf{n}$ , where  $\mathbf{n}$  denote the sequence of AWGN samples. Then the received bits  $y_{i,j}$  are hard-decided to the  $z_{i,j}$ , where  $z_{i,j} = 1$  if  $y_{i,j} \geq 0$  and  $z_{i,j} = 0$  otherwise. Finally, the received bits are decoded by using both parameters on the row and column directions as follow.

**Step 1:** Compute the syndrome  $s_m^{i,j}$  in every sequence on the row  $i$  and column  $j$  directions separately from

$$s_m^{i,j} = \sum_{n=1}^{N^r \times c} z_n H_{mn}. \quad (3)$$

where  $H_{mn}$  is the element on the  $m$ -th row and  $n$ -th column of the parity-check matrix  $\mathbf{H}^{\text{row}}$  and  $\mathbf{H}^{\text{col}}$  separately.

**Step 2:** Compute  $E_{i,j}$  of every bit on the 2-D codeword from

$$E_{i,j} = \frac{1}{|y_{i,j}|} \left[ \sum_{m \in M_{\text{row}}(j)} (2s_m^j - 1) \left( \sum_{j \in N_{\text{row}}(m)} |y_{i,j}| \right) + \sum_{m \in M_{\text{col}}(i)} (2s_m^i - 1) \left( \sum_{i \in N_{\text{col}}(m)} |y_{i,j}| \right) \right] \quad (4)$$

**Step 3:**  $z_{i,j}$  is flipped if  $(i, j) = \arg \max_{1 \leq i \leq N^r, 1 \leq j \leq N^c} E_{i,j}$ . Then the steps 1-3 are repeated until all of  $s_m^{i,j}$  equal 0 or the maximum number of iterations is reached.

## 4. Multiple bit flipping algorithm

Previously, the P-WBF algorithm will flip only the bit with the highest unreliable value at each iteration. Thus, when a large 2-D codeword is decoded by the P-WBF algorithm, large number of iterations and long decoding latency are required for the convergent performance. Therefore, in this work, we propose to use multiple-bits flipping to improve the decoding speed. The proposed algorithms can be divided into 2 distinct methods as follow.

### 4.1. Page-fixed weighted bit-flipping algorithm

For the page-fixed weighted bit-flipping (PF-WBF) algorithm, the same number of bits is flipped at each iteration. Let  $n$  be the number of flipped bits, where  $n \geq 2$ . The steps of PF-WBF algorithm are similar to those of the P-WBF algorithm, but the 3<sup>rd</sup> step are modified to

---

**Step 3:** The  $E_{i,j}$  values are sorted in a descending order. The  $n$  bits with the highest  $E_{i,j}$  are flipped. Then the steps 1-3 are repeated until all of  $s_m^{i,j}$  equal 0 or the maximum number of iterations is reached.

---

### 4.2. Page-threshold weighted bit-flipping algorithm

For the page-threshold weighted bit-flipping (PT-WBF) algorithm, the number of flipped bits will be changed following the threshold at each iteration. The steps of PT-WBF algorithm are similar to those of the P-WBF algorithm, but the 3<sup>rd</sup> step are modified to

---

**Step 3:** The bits with  $E_{i,j}$  above the threshold are flipped. Then the steps 1-3 are repeated until all of  $s_m^{i,j}$  equal 0 or the maximum number of iterations is reached.

---

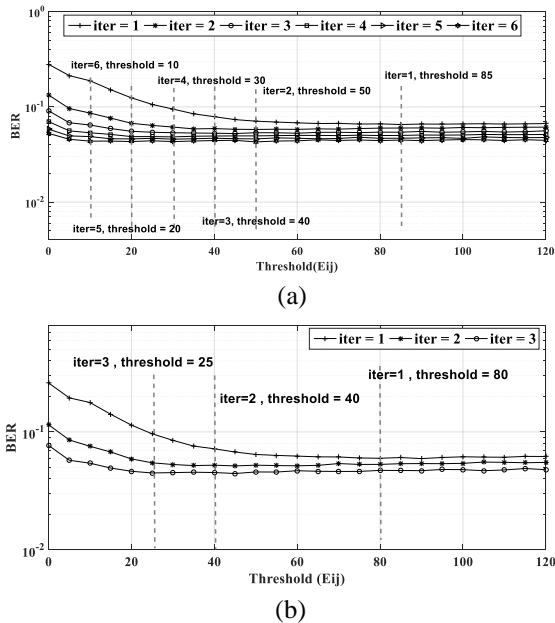


Fig. 5. The threshold for AWGN (a) and TDMR (b) channel.

In Fig. 5, the optimal thresholds of the PT-WBF algorithm are investigated. The size of 2-D codeword is  $500 \times 500$  bits. The column-weight ( $d_c$ ) and code-rate are 3 and 0.5, respectively. In the AWGN channel, the minimum BER will be given when the threshold equals 85 at the first iteration. Therefore, when the  $n$  bits with  $E_{i,j}$  values more than 85 are flipped at first iteration, both the minimum BER and decoding speed-up are achieved. We can list the optimal thresholds for PT-WBF decoding algorithm in Table 1. Obviously, the thresholds for the AWGN and TDMR channel are specially used for 6 and 3 iterations, respectively. Then the  $n$  value are set to 1.

Table.1 the optimal threshold for PT-WBF decoding algorithm

Channel	Iter = 1	Iter = 2	Iter = 3	Iter = 4	Iter = 5	Iter = 6
AWGN	85	50	40	30	20	10
TDMR	80	40	25	-	-	-

## 5. Simulation results and discussions

In this section, the BER performance of P-WBF, PF-WBF and PT-WBF algorithm are compared in the AWGN and TDMR channels. The size of 2-D codeword is  $500 \times 500$  bits. The column-weight ( $d_c$ ) and code-rate are 3 and 0.5, respectively. For the TDMR channel, the equalizer is designed by the minimum mean square error (MMSE) criterion [9]. We use equalizer with 11 taps and the length of GPR target is equal to 3.

The BER performances of P-WBF, PF-WBF and PT-WBF algorithms after 3,000 iterations are compared in Fig.6. The performances of PF-WBF algorithm with  $n = 3, 5, 7$  and  $9$  are better than those of the P-WBF algorithm. The coding gains are 1.9 dB, 2.9 dB, 3.5 dB and 3.9 dB, respectively. Furthermore, the PT-WBF algorithm can achieve a 3.6 dB coding gain over the P-WBF algorithm. Although the performances of both proposed algorithms are better than those of the P-WBF algorithm at small iterations, its performances will suffer at high iterations as shown in Fig.7.

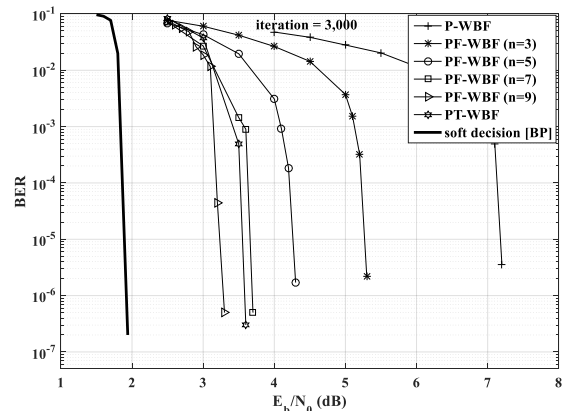


Fig. 6. The BER performances of P-WBF, PF-WBF and PT-WBF in an AWGN channel after 3,000 iterations.

Figure 7 compares the BER performances of P-WBF, PF-WBF and PT-WBF algorithm at the convergent performance. The PT-WBF and PF-WBF algorithm with  $n = 3$  and  $5$  are worse than the P-WBF algorithm. Whereas,

the performances of the PF-WBF algorithm with  $n = 7$  and  $9$  are comparable to the P-WBF algorithm.

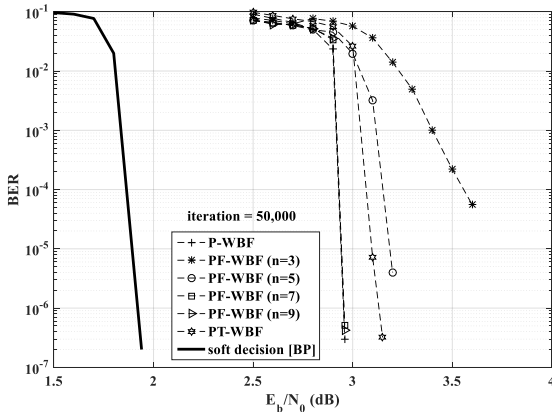


Fig. 7. The BER performances of P-WBF, PF-WBF and PT-WBF in an AWGN channel after 50,000 iterations.

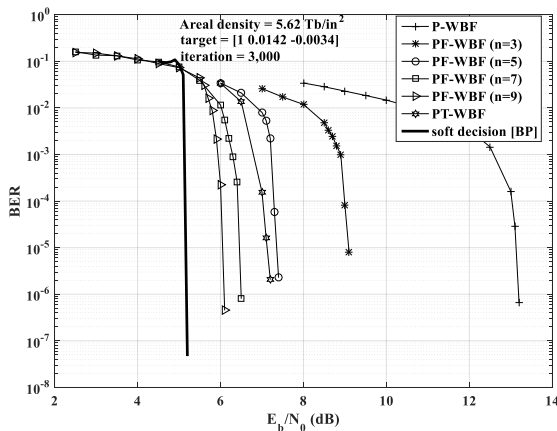


Fig. 8. The BER performances of P-WBF, PF-WBF and PT-WBF in the TDMR channel after 3,000 iterations.

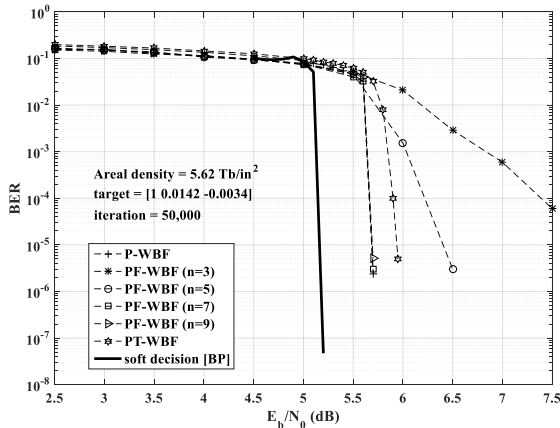


Fig. 9. The BER performances of P-WBF, PF-WBF and PT-WBF in the TDMR channel after 50,000 iterations.

The BER performances of P-WBF, PF-WBF and PT-WBF algorithm in the TDMR channel with an areal density of  $5.62 \text{ Tb/in}^2$  have been shown in Fig. 8 and 9. At the small iteration numbers, the performances of P-WBF, PF-WBF and PT-WBF algorithm after 3,000 iterations are compared in Fig. 8. The PF-WBF algorithm with  $n = 3, 5, 7$  and  $9$  can achieve  $4.1 \text{ dB}, 5.8 \text{ dB}, 6.7 \text{ dB}$  and  $7.1 \text{ dB}$  coding gains over the P-WBF algorithm. Similarly, the PT-WBF can achieve a  $5.9 \text{ dB}$  coding gain over the P-WBF algorithm.

When the BER performances of P-WBF, PF-WBF and PT-WBF algorithm are compared at the convergent performance, the performances of both proposed algorithms are not better than those of the P-WBF algorithm as shown in Fig. 9. The PT-WBF and PF-WBF algorithm with  $n = 3$  and  $5$  are still worse than the P-WBF algorithm. The performances of PF-WBF with  $n = 7$  and  $9$  are still comparable to the P-WBF algorithm. However, the performances of P-WBF, PF-WBF and PT-WBF which is hard-decision algorithm are always worse than those of the optimal soft-output BP decoding or soft-decision algorithm.

## 6. Conclusions

In this research, we propose the page-based weighted bit-flipping (P-WBF) decoding with multiple-bits flipping technique for product LDPC codes. Two distinct methods based on fixed and variable number of flipped bits, we coined the term PF-WBF and the PT-WBF algorithm, respectively. The BER performances of P-WBF and proposed algorithms are compared in the AWGN and TDMR channels. The simulation results show that the performances of two proposed algorithms are always better than those of the P-WBF algorithm at small iteration number, but they will suffer at high iterations.

## 7. Acknowledgment

The authors gratefully acknowledge the financial support from research and researchers for industries (RRI) under grant no. MSD57I0153, the Thailand research fund (TRF) and Western digital (Thailand) Co. Ltd.

## References

- [1] R. Wood, M. Williams, A. Kavcic and J. Miles, "The feasibility of magnetic recording at 10 terabits per square inch on conventional media", *IEEE Trans. Magn.*, vol. 45, no. 2, pp. 917-923, 2009
- [2] M. Kryder, E. C. Gage, T. W. McDaniel, W. A. Challener, R. E. Rottmayer, G. Ju, Y.-T. Hsia and M. F. Erden, "Heat assisted magnetic recording", *Proc. IEEE*, vol. 96, no. 11, pp. 1810-1835, 2008.
- [3] H. J. Richter, A. Y. Dobin, O. Heinonen, K. Z. Gao, R. J. M. v. d. Veerdonk, R. T. Lynch, J. Xue, D. Weller, P. Asselen, M. F. Erden and R. M. Brockie, "Recording on bit-patterned media at densities of  $1 \text{ Tb/in}$  and beyond", *IEEE Trans. Magn.*, vol. 42, pp. 2255-2260, 2006.
- [4] Z. Qi, N. C. Sum, LDPC product codes, *The Ninth International Conference on Communication Systems (ICCS)*, pp. 481-483, 2004.
- [5] S. Khittiwitachayakul, W. Phakphisut and P. Supnithi "Weighted bit-flipping decoding for product LDPC codes", *International Conference on Electrical Engineering/Electronics, Computer, Telecommunications and Information Technology*, June 2016.
- [6] K. S. Chan, et al., "TDMR Platform Simulations and Experiments", *IEEE Trans. Magn.*, vol. 45, no. 10, October, 2009.
- [7] M. Yamashita, "R/W Channel Modeling and Two-Dimensional Neural Network Equalization for Two-Dimensional Magnetic Recording", *IEEE Trans. Magn.*, vol. 47, no. 10, October, 2011.
- [8] S. Kobayashi, "The frontiers of real-coded genetic algorithm", (*in Japanese*) *J. Jpn. Soc. Artif. Intell.*, vol. 24, no. 1, pp. 147-162, 2009.
- [9] J. Moon and W. Zeng, "Equalization for maximum likelihood detector", *IEEE Trans. Magn.*, vol. 31, pp. 1083-1088, March, 2009.
- [10] D. J. C. MacKay, and I. N. Neal, "Near Shannon limit performance of low-density parity-check codes", *Electronics letters*, vol. 32, pp. 1645-1646, 1996.
- [11] C. H. Lee, and W. Wolf, "Implementation-efficient reliability ratio based weighted bit-flipping decoding for LDPC codes", *Electronics letters*, vol. 41, pp. 755-757, 2005.